The Electrochemical Behaviour of Steel Reinforced Concrete During Accelerated Corrosion Testing

S.A. Austin[*]*, R. Lyons, M.J. Ing*

Centre for Innovative Construction Engineering, Loughborough University, Leicestershire, LE11 3TU, UK.

ABSTRACT

Corrosion of reinforcing steel presents a major durability issue worldwide and is the focus of much research activity. The long time periods involved in replicating reinforcement corrosion within laboratories has resulted in a number of accelerated test methods being developed. The basis of this research presented in this paper was to examine the impressed current technique often used to induce reinforcement corrosion. The suitability of the technique to model chloride induced corrosion was investigated by examining the electrochemical nature of the test method. Corrosion was induced in prisms of differing characteristic strengths and cover thicknesses by applying a current for between 3 and 17 days. The gravimetrical and theoretical mass losses are compared and a modified expression based on Faraday's law relating the electrical current to the mass loss is also proposed which accounts for the localised nature of chloride-induced corrosion. It was found that the technique is a suitable method to simulate reinforcement corrosion.

Keywords: *Corrosion, Electrochemical properties, Acoustic Emission, Acceleration*

* Corresponding author. Fax: +44 1509 223981
E-mail address: S.A.Austin@lboro.ac.uk
Telephone: +44 1509 222608

INTRODUCTION

Research Significance

The focus of this paper is to examine and review the impressed current method of accelerating chloride induced corrosion. Whilst this method is common, little published work has been found describing its suitability as a technique to model reinforcement corrosion and the theory behind the practice. In particular, the electrochemical implications of applying an external current are examined and compared against the natural electrochemistry of corrosion of steel reinforcement. The experimental programme investigated the applicability of applying Faraday's Law for the calculation of mass loss under the test conditions set out below and the paper discusses the suitability of the technique as a model for accelerating chloride-induced reinforcement corrosion within the laboratory. Corrosion induced by an impressed current was detected with a novel corrosion detection technique based on acoustic emission.

Corrosion Mechanisms

The damaging role that corrosion of reinforced concrete has on the durability of concrete structures is well documented[1,2]. To improve understanding of reinforcement corrosion and its effects, accelerated modelling of corrosion in the laboratory is often required. The reliability and accuracy of the results will depend upon the closeness of the laboratory simulation to corrosion in real-life. Good quality concrete will normally offer excellent chemical protection for the steel reinforcement against corrosion[3] due to the high alkalinity and the low permeability of the matrix[4]. At a pH of 13.5, the interaction between the

steel and the hydroxyl ions present in the pore solution results in the formation of an insoluble γ–Fe_2O_3 layer, rendering the underlying metal passive. The low permeability of the concrete represents the ability of the concrete matrix to resist diffusion of aggressive species, such as the chloride ion, into the concrete[4].

Neither the high alkalinity of the pore solution or the low permeability of the cover can guarantee that the steel will resist corrosion, especially in aggressive environments such as marine structures. Chloride ions may enter the concrete during mixing, as admixtures, or after curing from external sources such as sea-water and de-icing salts. Once chlorides have reached bar level, they depassivate the embedded steel by locally breaking down the protective layer[5,6]. The time chloride ions take to reach the level of the reinforcement depends on the mechanism of intrusion, the external concentration of the chlorides and the internal microstructure of the concrete[7]. In water-saturated concrete, chlorides are considered to penetrate the cover by a diffusion mechanism with the driving force being differential concentration gradients[7]. In this circumstance, Fick's second Law of Diffusion can be applied to model the rate of chloride penetration. In partially saturated concrete, chlorides enter by adsorption and capillary forces[7,8] and the period of intrusion is generally known as the initiation period. This is followed by propagation of the corrosion, the duration being controlled by factors such as temperature, oxygen concentration and moisture content. At low corrosion rates, of the order $1\mu A/cm^2$, it is estimated that the propagation period may continue for 20 years before cracking of the cover occurs[9].

To study the effects of corrosion within a realistic time-scale, it is sometimes necessary to accelerate the initiation period and occasionally control the rate of corrosion during the propagation stage. The methods employed to do this will vary upon the nature of corrosion under investigation. For example, to accelerate carbonation induced corrosion, the concrete can be placed in a CO_2 chamber at 50% RH to rapidly increase neutralisation of the pore water[10,11].

Accelerated chloride induced corrosion techniques are frequently used to reduce the time taken for a critical level of chlorides to reach the reinforcement bar[12-17]. Three methods are common; admixed chlorides, impressed voltage/current and wet/drying techniques. The latter usually requires several months before sufficient levels of chloride ions have permeated the cover to cause depassivation as the extent of the movement of salt will depend on the duration of the wetting and drying periods[6]. Furthermore, the subsequent rate of corrosion is not accelerated and is dependent upon a sufficient supply of oxygen and water. The first two methods are either combined or separate, depending upon the reason behind the study.

Where an impressed current is used to drive corrosion, the amount of mass loss is related to the electrical energy consumed once passivity has been compromised, and can be modelled using Faraday's law, Equation [1].

$$Mass\ Loss = \frac{Mit}{zF} \qquad (1)$$

Where M = molar mass (55.847 g/mol for iron)

i = current (A)

t= time (s)

z = number of electrons transferred

F = Faradays constant (96,487Coulombs/mole)

Electrochemistry of corrosion

Corrosion is an electrochemical reaction involving the transfer of charge from one species to another. It consists of two half-cell reactions, an anodic reaction and cathodic reaction, connected together by an electrolyte. To maintain a charge balance the rate of reduction (anodic) and rate of oxidation (cathodic) must be equal[3].

Steel, when in the presence of water and oxygen will undergo a reduction reaction at the anode where the exact nature of this reaction is dependent upon the reaction thermodynamics. For example, iron can dissolve to form Fe^{++}, but can also form stable oxides that in some instances may protect the underlying steel (such as the passive layer). All the possible oxidation reactions between iron and water have been measured and calculated by Pourbaix[18] and presented in a Potential-pH diagram, which illustrates the thermodynamically stable phases of the possible reactions as a function of electrode potential, and pH, giving rise to various zones of corrosion, passivity or immunity.

At a pH of 13.5, two solutions generally apply for iron: passivity or immunity as shown in Figure 1. Immunity is only obtainable by lowering the potential

below the equilibrium potential of hydrogen (line a), achieved by applying external energy to the reaction (cathodic protection). At potentials more positive than –1125 mV Standard Calomel Electrode (SCE) the steel is covered by a stable film of Fe_3O_4 or Fe_2O_3 which reduces corrosion of the active underlying metal to a negligible rate ($0.1\mu A/cm^2$). Consequently, the potential of passive steel can vary between –1125 mV to +175 mV SCE (the equilibrium potential of O_2 at pH 13.5), governed by the pH of the pore solution and the oxygen content at the rebars, as shown in the cathodic Nernst Equations[19] [2,3].

$$E_c = E^o + \frac{RT}{4F} \ln a_{O_{2\,(dis)}} \qquad [2]$$

$$E_c = +1.22 - \frac{0.059}{4} pH \qquad [3]$$

Where: E_c = Cathodic potential (mV)

E^o = Open potential (mV)

R = Molar Gas constant

T = Absolute Temperature (K)

a = activity

The mixed potential (E_{corr}) measured in any corroding solution is a combination of the anodic and cathodic reaction, governed by the mixed potential theory. Both reactions are polarised towards each other as shown schematically in Figure 2a. This corresponds to a potentiostatic curve for steel in an alkaline solution showing three regions of interest: general corrosion, passivity and oxygen evolution. E_{corr} is equal to the intersection of the anodic

and cathodic polarisation curves. Each valve of E_{corr}, has a corresponding current value (I_{corr}). However, this value is only apparent, as no net current exists due to the balance of charge.

In non-carbonated, chloride-free concrete, the pH is usually fairly constant over time, and variations in the potential are usually as a result of the changing oxygen content at the steel-concrete interface. At very low oxygen levels, the potential (E_{corr}) can fall to very negative values (Figure 2b) where the passive layer is no longer stable and may be reduced leaving the steel surface in an active state. However, the corrosion rate in these circumstances is reported to be not much greater than when passive[3].

EXPERIMENTAL PROCEDURE

Experimental Details

The experimental methodology was as follows. Corrosion of the rebar was induced by applying a fixed anodic current of 100μA/cm^2 to the prisms. The electrochemical potential of the steel was monitored periodically using a saturated calomel reference electrode placed on the concrete surface. Due to the effect of the applied voltage on the potential, corrosion activity was continuously monitored using the novel acoustic emission technique. Upon completion of the test, the prisms were visually examined for surface cracking and a visual inspection of the corroded area was undertaken. The gravimetric mass change was recorded after the rebar was removed from the prism and cleaned.

Singly reinforced concrete prisms were cast with designed characteristic strengths of 20, 35 and 50 MPa. All mixes contained uncrushed river gravel with a maximum aggregate size of 10 mm and had a free-water content of 180 kg/m^3. The mix proportions for each strength are shown in Table 1, together with the target strengths. All mixes used Type 1 Portland Cement. The average strength of the C20 mix was 32 MPa with a range of 27-36 MPa and an average standard deviation coefficient of 11%. The average strength of the C35 mixes were 54 MPa with a range of 47-60 MPa and an average standard deviation coefficient of 6% (3.6-10). The C50 mix had a mean strength of 68 MPa (range 60-75) with a standard deviation coefficient of 9%.

The prisms contained one ordinary grade 460 deformed steel rebar having a nominal diameter of either 12,16 20 mm placed so that the cover was equal on three sides. The thickness of the cover (c) was intentionally varied between 16, 25, and 40 mm (±1mm). The dimensions and properties of individual prisms are given in Table 2. The last 20 mm of each bar end was wrapped in electrical insulation tape prior to casting to eliminate edge effects. Before casting, the reinforcing bars were wire brushed to remove any scale and then weighed to a precision of two decimal places. The prisms were water cured for 28 days, then stored in laboratory conditions of 20^{o}C +/- 5^{o}C for a minimum of 28 days before testing.

In any one test, three prisms, each of the same type, were placed in a corrosion cell as shown in Figure 3. A 24-hour period passed before the current was passed through the cell. Acoustic Emission (AE) readings were taken during

this initial 24 hour period to establish background levels of emission for each prism. A 30VDC / 2A power supply was set to constant current mode supplying an anodic current of 100 $\mu A/cm^2$ to each rebar. This current density is reported as being the maximum corrosion current found in real conditions[20] and has been used by several researchers[20,21]. Electrical continuity was provided by a wet wick saturated in a 5% sodium chloride solution. The counter electrode was an AISI 304 stainless steel plate immersed in the electrolyte. The half-cell of the concrete was recorded initially and then periodically throughout the test duration. Termination of the test occurred between 1 – 3 days after the initiation of corrosion activity was detected by the AE. This gave a range to the extent of corrosion. In a few instances the test was terminated approximately one day before it was expected AE would start, to verify that corrosion was not occurring prior to the onset of characteristic emissions.

A fourth control prism from the same batch, without an impressed current, was used as a control and monitored continuously for the duration of the test to establish the background noise levels associated with the testing environment and the concrete. Upon completion of the test, the control beam was opened to check that there was no visible corrosion of the rebar and hence confirm that in the absence of any significant AE corrosion was not occurring.

On completion of the test, the prisms were photographed and examined for any evidence of external cracking. The prisms were then sliced in half on either side of the rebar with a diamond saw. The rebar was removed and the

total area of corrosion products calculated after measuring with a rule marked in 0.5mm divisions. Finally the bars were wire brushed to remove any corrosion products and re-weighed. Mass loss was also calculated theoretically and compared to the gravimetric value.

Detection of Corrosion Activity

A technique was required that would not interfere with or be affected by the applied current, and could be used continuously so that a reasonably accurate estimate of corrosion initiation could be made. Application of AE to the detection of corrosion induced concrete damage has been reported as being a suitable laboratory tool[22]. Furthermore, it is reported to be sufficiently sensitive to detect corrosion related deterioration processes at an early stage[23]. The use of this technique is not widely practised and relatively little information has been published of its use as a laboratory tool. However, previous work has found that this non-destructive technique was able to detect active corrosion before traditional methods such as half-cell and galvanic current measurements[24-25]. The ability of this technique to detect early age corrosion without perturbation of the corrosion cell is a clear advantage over other methods. Acoustic emissions are generated as a consequence of microcrack development and their propagation in the concrete during the discharge of corrosion products[26-27].

The AE DiSP[†] 4-channel board was used with piezoelectric transducers connected in series to an external pre-amp. Both hit and time driven data were

[†] Supplied by Physical Acoustics Limited

recorded onto a hard drive for post processing. The transducer was attached directly to the top of the prism, using adhesive grease as a couplant.

RESULTS

Half Cell Potentials

Half-cell potentials taken during the initial 24-hour period ranged between –90 to 120 mV SCE, placing the bars within the passive region. This was confirmed by the absence of significant acoustic emissions. This is the usual state for non-carbonated, chloride-free concrete.

When the anodic current was applied to the rebar, the half-cell reading value shifted to extremely positive values in the range of +550 to 1455 mV (SCE). This was not accompanied by any noticeable increase in AE. The rate of AE emission and half-cell potentials remained reasonably constant for between 2-17 days dependent upon the cover thickness, after which time a sudden increase in acoustic emissions occurred and in some instances a small drop in the electrochemical potential.

Breaking open a prism approximately one day before an increase in AE revealed that the rebar showed no evidence of corrosion on the metal surface despite the very positive half cell potential. However, opening the sample one to two days after the onset of emission revealed corrosion of the rebar surface in all cases. This confirms firstly that the AE technique is a good method for detection of corrosion in reinforced concrete and secondly, steel remains

passive at high potentials in the absence of any aggressive specie. A typical example of the increase in AE is shown in Figure 4.

An understanding of the electrochemical influence involved in impressing an anodic current can be obtained from Figure 5. At low potentials, line AB, general corrosion of the steel occurs with increasing current density until the primary passive potential (E_{pp}) is reached. This potential corresponds to a sudden drop in current density which can be of several orders of magnitude, corresponding to the formation of a very thin passive film (line CD)[28]. The oxide formed in this manner protects the underlying steel even at very positive potentials. At potentials greater than the transpassive potential (E_{tp}) the oxidation reaction that occurs corresponds to an oxidation of water to oxygen, where E_{tp} is the equilibrium potential between water and oxygen [29].

The passive oxide present on the steel is a conductor of charge, therefore, it is only able to maintain a small potential difference (~ 1V)[28] across the passive film, significantly less than the potential applied to achieve the desired current density. Consequently, impressing a current raises the potential on the pore water side of the film to a more noble value within the oxygen evolution potential range[28]. Figure 5 shows the shift from equilibrium values (E_{corr} and I_{corr}) necessary to obtain the desired current density. The potential difference ($E_{applied}$) must be supplied by an external source and can be expressed as shown in Equation [4].

$$E_{applied} = (E_a' - E_{corr}) + (E_{corr} - E_c') \qquad [4]$$

Where E_a' is the imposed anodic potential and E_c' is the imposed cathodic potential.

Polarisation

Polarisation of the rebar also induces a second reaction, which under the test conditions eventually results in the corrosion of the rebars. It is well reported that chlorides move quicker through concrete when an electrical field is applied between an area of low chloride concentration and an area of high concentration[30-32]. The thickness of the concrete and the applied voltage influences the depth of penetration of chlorides over a period of time[33]. Within the scope of the experiment, the thickness of the concrete varied between 16, 25 and 40 mm and the applied voltage was a function of both the resistivity of the concrete and the water cement ratios associated with the different strengths. The source of the chloride ion was the electrolyte.

In concretes where chlorides are present, a fourth region is introduced into the Potential-pH diagram (Figure 6) denoting the range of potentials and pH over which pitting corrosion is possible. This introduces a rupture potential, E_r, on the anodic polarisation curve at which passivity breaks down and localised corrosion can initiate on the rebar surface. At low concentrations of chlorides, E_r may exist at high potential values, thus corrosion of depassivated areas might occur concurrently with oxygen evolution where passivity is intact. In Figure 7, the half-cell values have been plotted together with the AE cumulative energy over the duration of the test for a representative beam. AE

energy is measurement in atto Joules of the energy contained in each hit. Figure 7 clearly shows the change in potential imposed by applying the current to the rebar. It is also evident that the potential remains fairly constant until the end of the test where the value falls, corresponding with a sudden increase in AE. The imposed potential is always greater than line a, corresponding to E_{tp} for steel in a solution of pH 13.5.

Figure 8 illustrates the effect of cover thickness on the time taken for corrosion to initiate at an applied current density of 100 μA/cm^2. It is apparent that the cover thickness has a significant influence on the time until corrosion initiates, which may be related to the diffusion of the chloride ion. It was assumed that initiation of corrosion would be immediate in the case of zero cover, where access to chlorides is unrestricted. The applied voltages were in the range of 2.98 – 7.25 volts, with an average of 4.7 volts. No correlation between voltage and strength or cover thickness was observed.

Corrosion

Localised breakdown of passivity combined with high imposed anodic potentials can result in severe localised corrosion of the rebar, confirmed by the experimental work. The percentage of surface corrosion ranged between 0.2 – 39.8%, with a median value of 4.9%. Corrosion products were typically located on the underside of the rebar, supporting the argument that corrosion was initiated due to the presence of chlorides as this was the closest point to

the proceeding chloride front, assumed to be migrating through the cover under the influence of the applied electric field.

With the exception of the three bars that had a corroded area greater than 16%, the extent of corrosion was generally low as a result of terminating the test within a short time after initiation was indicated by the AE. Consequently, potentials in all cases remained consistently greater than E_{tp} (Figure 7) implying that oxygen evolution was probably occurring where passivity was still intact and anodic dissolution was occurring where passivity had been compromised. This suggested a split in the applied current used for the oxidation of water and steel.

The split anode reactions will influence the theoretical mass loss calculated using Equation [1]. A more reliable estimate of steel loss requires a modification to the terminology used in Faraday's Law. The variable *time*, measured in seconds is not the total time duration of the applied current, but the *duration* (d_c) of the corrosion activity from the start of depassivation, identified by the onset of AE, to the termination of the test. Secondly, the value used for the *current*, must be proportional to the area of the steel on the bar that has been depassivated (a_c) and not the whole surface area (A_e). This assumes that equal charge is used in the reduction of oxygen as in the dissolution of steel and that the area covered in corrosion products has depassivated. The modified version of Faraday's law, developed for this work, is expressed in Equation [5]:

$$Theoretical\,Mass\ Loss = \frac{Mid_c a_c}{A_e zF} \qquad [5]$$

The ratio of theoretical and gravimetric mass losses obtained from Equations [1] and [5] has been plotted in Figures 9 and 10. Good agreement (i.e. an approximate ratio of unity) is evident in Figure 9 where passivity has been taken into account, whereas in Figure 10 the mass loss has been over estimated by a factor between 4 to 200. Over estimations have been reported by Auyeung *et* al[14], similarly other workers[34] observed under estimations when the impressed current was continued for a significantly longer period (70-221 days) and the concrete contained admixed chlorides promoting general corrosion. An element of scatter is still apparent in Figure 9 due to the physical errors inherent in obtaining both mass loss values. The mass loss as a result of passivity was considered to be negligible during the relatively short experimental period and has been discounted.

DISCUSSION

Suitability of the impressed current technique

Impressing an external current to accelerate the corrosion of steel in concrete has been shown to reliably induce corrosion of the reinforcement. The analysis presented has been based upon the Pourbaix diagram and Pourbaix's theoretical potentiostatic curves for steel in a solution at pH 13.5[29]. Whilst they provide a sound thermodynamic basis for understanding the corrosion reactions, their interpretation is limited to a rough guide as the basis of the graphs originate from pure metals in pure, stirred solutions thus do not

consider the possible effects of restricted mass transfer; therefore inherent differences exist between the two.

The primary objective of any accelerated technique should be to resemble naturally induced corrosion in terms of the type of corrosion products and method of attack. However, the similarities and deviations between the two mechanisms must also be considered to enable a decision regarding its effectiveness as a technique to be made.

When an external electric field is applied to passive concrete, electrolysis of the pore water can occur at both electrodes[7]. At the anode, the reaction previously discussed, involving the evolution of oxygen, also generates hydrogen ions which diffuse into the pore water adjacent to the rebar lowering the local pH[35]. A reduction in the pH can lower the critical chloride concentration required to induce corrosion[36], therefore chloride content analysis results may not be directly comparable to non-impressed tests, hence these were not recorded.

The impact of the localised changes in pH on the steel will depend upon the mobility of the hydrogen ions, which can migrate from the rebar surface under the action of the electric field, differential concentration gradients[35], or be diluted by the OH^- reserves in the matrix. The stability of the passive film in the absence of chlorides is dependent upon the pH of the adjacent pore water. If significant electrolysis occurs, the local reduction in pH induced by hydrolysis may be sufficiently large to fall below the values required to

maintain passivity of the steel[37]. To investigate this possibility, a phenolphthalein solution was sprayed onto an area of concrete, which had been in immediate contact with the rebar at a location where corrosion had not occurred. The results obtained from the several beams tested indicated that at termination of the test the pH of the concrete in immediate contact with the steel remained sufficiently alkaline to support passivity; hence any change in the pH of the pore solution due to electrolysis was not considered to be significant to the durability of passivity over the relatively short test durations and within the applied voltage range. This is also supported by Grimes *et al*[38] who found that the pH of the concrete adjacent to non-corroded steel, having undergone impressed current corrosion tests, was 11.9-12.1.

It is generally accepted that the acidity produced during chloride-induced corrosion results in the formation of soluble oxides, which diffuse away from the anode to areas of lower pH within the cement matrix. The corrosion product found on the rebars upon opening was typically a 'wet' green / black oxide paste with a brown oxide on the periphery. On exposure to the air, the green oxide turned into a 'rust red' colour. The green/black colour and phase of the oxide would suggest the oxide was a type of iron chloride complex, formed as an intermediate stage of chloride-induced corrosion[6,39]. Oxides were also present at the concrete / steel interface exhibiting the start of oxide migration into the cover. In a few cases, a longer duration of applied current enabled oxides to diffuse further into the bulk matrix, typically around aggregates as opposed to through the paste, where they had precipitated into a solid orange oxide, probably due to the alkaline environment. Such action

closely models the behaviour of oxides in real structures where chloride-induced corrosion is characterised by localised rust stains on the surface which can often be observed in deteriorating structures. It is the formation of these higher oxides states that have a large increase in volume, which induces the major stresses in the cover, eventually cracking the concrete[40].

Whilst attack along the length of the beam was localised, the morphology of the attack on the active areas on the rebars resembled general corrosion. This may be due to the electro-migration of the chlorides to this region forming a sufficient quantity of chlorides to induce general corrosion or, as the authors suspect, due to the early termination of the test whilst corrosion was at a pre-pitting stage. In trial experiments, the current was impressed for longer durations resulting in pitting of the steel. In work undertaken by Gonzalez *et al*[20] corrosion was continued for a significantly greater duration (1 month), under the action of an impressed current where pitting corrosion was reported. They also stated that the impressed current technique produced R values, (defined as the ratio of maximum penetration to average penetration) similar to, although slightly higher than those obtained under non-impressed conditions.

The primary electrochemical difference of this technique to naturally corroding systems is the raising of the potential to a value greater than E_{tp}, where the corrosion rate does not correspond with an equilibrium mixed potential or a potential obtainable under usual service conditions without applying an external source of energy. Hence, imposing such a potential will

result in the steel being in an artificially polarised state. Whilst this had no apparent effect on the bars even after a 17-day period, a gradual reduction in the pH due to electrolysis might occur together with migration of other ions which may accelerate the degradation process[41] if continued over an extended time period.

The impressed current method of corrosion acceleration has many advantages in addition to the obvious savings in time and money. One advantage over other accelerated techniques is the ability to control the rate of corrosion, which usually varies due to changes in the resistivity, oxygen concentration, and temperature. Any change in one of the variables would be compensated for. For example, a change in the resistivity of the concrete as a result of temperature fluctuations or evaporation of the pore water can be counter-balanced by supplying a greater voltage, thereby maintaining the desired corrosion rate. This removes much of the variation encountered in corrosion measurements with time.

Whilst the corrosion rate is fixed, the area of steel depassivated and corroding cannot be controlled due to the preferential flow path of chlorides between the aggregate/cement interface[33] and the existence of preferential areas along the bar surface due to geometrical heterogeneitys[42]. Consequently, the total mass loss varied between samples. The geometry of the corrosion cell was such that depassivation occurred on the underside of the rebar, closest to the electrolyte, against the direction of gravity.

In comparison with naturally induced corrosion, the technique differs in so much that the potential of the passive rebar during the initial stages is far removed from the natural potential range. Furthermore, the subsequent corrosion rate is not governed by the mixed potential theory but by the applied current. The applied current compensates for the consequential discrepancy between the anodic and cathodic potentials and offers the benefit of reducing the sensitivity to changes in oxygen content, moisture content or temperature as occurs naturally. This enables good control over the corrosion rate for experimental purposes.

CONCLUSIONS

The scientific justification for accelerating corrosion using an impressed current is strong, dramatically reducing the initiation period required for depassivation from years to days and fixing the desired rate of corrosion without compromising the reality of the corrosion products formed. Based on the experimental work and argument presented, the following conclusions may be drawn.

1. The impressed current technique has been confirmed to be an effective and quick method of accelerating chloride-induced corrosion. However,

electrochemistry behind the mechanism differs from naturally induced corrosion.

2. Accounting for oxygen evolution and passivity when applying Faraday's law was shown to significantly improve the correlation between theoretical and gravimetrical mass loss.
3. Oxygen is assumed to be evolved from the applied current in the absence of chloride ions
4. The acoustic emission technique was effective and reliable at detecting the onset of corrosion. This view is supported by good prediction of mass loss by Faraday's law taking into account the passive period indicated by the AE measurement.
5. The thickness of the concrete cover had a greater influence than the concrete strength on the time required for chlorides to permeate through the cover.
6. During the first few days of testing, the corrosion was restricted to a small number of sites on the bar surface, similar to naturally induced corrosion.
7. The orientation of the specimen, with depassivation occurring on the underside of the bar, was not conducive to pit formation.

ACKNOWLEDGEMENTS

This work was undertaken at the Centre for Innovative Construction Engineering, Loughborough University. The authors acknowledge the financial assistance from the EPSRC and Balvac Whitley Moran Ltd in addition to specialist equipment loan and technical assistance from Physical Acoustics Limited. Atkins Consultants Ltd also gave assistance.

REFERENCES

1. B. Boyard, C. Warren, S. Somayaji R. Heidersbach, ASTM STP 1065, "Corrosion rates of steel in concrete," eds N.S. Berke, V. Chaker, (Whittington,. Philadelphia, P.A: ASTM, 1990), p. 174.
2. RILEM, Mater. Struct. 9, 51 (1976): p. 187.
3. C.M. Hansson, Th. Frolund, J.B. Markussen, Cem. Concr. Res. 15 (1985): p. 65.
4. P.S. Mangat, B.T. Molloy, Mater. Struct. 25 (1992): p. 404.
5. C.L. Page, P. Lambert, P.R.W. Vassie, Mater. Struct. 24 (1991): p. 243.
6. A.M. Neville, Mater. Struct. 28 (1995): p.63.
7. C. Andrade, Cem. Concr. Res. 23 (1993): p.724.
8. M.G. Grantham, M.J. Gray, J.P. Broomfield, "Chloride diffusion modelling and corrosion rate data for lifetime prediction in marine, highway and car parking structures," in Proc. Seventh International Conference on Structural Faults and Repair, ed. M.C. Forde (London, UK, 1997), p. 275.
9. C. Andrade, C. Alonso, A. Molina , Mater. Struct. 26 (1993) p. 453.
10. J.A. Gonzalez, S. Algaba, C. Andrade, Br. Corros. J. 15, 3 (1980) p.135.
11. N.I. Fattuhi, Cem. Concr. Res. 18 (1988) p. 426.
12. S. Ahmad, B. Bhattacharjee, R. Watson, ACI Mater. J. 94 (1997): p. 311.
13. G.J. Al-Sulamimani, M. Kaleemullah, I.A. Basunbul, Rasheeduzzafar, ACI Struct. J. 87 (1990): p. 220.
14. Y. Auyeung, P. Balaguru, L. Chung, ACI Mater. J. 97 (2000): p. 214.
15. J.G. Cabrera, Cem. Concr. Comp. 18 (1996): p. 47.
16. W.H. Hartt, "Laboratory method for corrosion testing of reinforced concrete using impressed current," CORROSION/79, Paper no. 133, March 1979.
17. ASTM G109, "Test method for determining the effects of chemical admixtures on the corrosion of embedded steel reinforcement in concrete exposed to chloride environments," (Amer. Soc. Testing Mat. Philadelphia, PA 1993).
18. M. Pourbaix, Atlas d'equilibres electrochemiques, 307 (Gauthier-Villars, Paris, 1963).
19. S.C. Das, "Computer-aided quantitative interpretation of electropotential survey results for RC structures," In Proc. Sixth International Conference on Structural Faults and Repair, ed. M.C. Forde, (London, UK, 1995), p. 209.
20. J.A. Gonzalez, C. Andrade, C. Alonso, S. Feliu, Cem. Concr. Res. 25 (1995): p. 257.
21. R.L. Miller, W. Hartt, Mater. Perfor. (1996) p. 20.
22. M.S. Weng, S.E. Dunn, W.H. Hartt, R.P. Brown, Corrosion 38, 1 (1982): p. 9.
23. S.E. Dunn, J.D. Young, W.H. Hartt, R.P. Brown, Corrosion 40, 7 (1984): p. 339.
24. Z. Li, F. Li, A. Zdunek, E. Landis, S.P. Shah, ACI Mater. J. 95 (1998): p.68.
25. A.D. Zdunek, D. Prine, " Early detection of steel rebar corrosion by acoustic emission monitoring," ITI Technical Report No. 16. 1995.

26. H. Idrissi, A. Limam, J. Acoustic Emission 18 (2000): p. 307.
27. M.J. Ing, S.A. Austin, R. Lyons, Paper submitted to Cem. Concr. Res. October (2002).
28. J.C. Scully, "The fundamentals of corrosion," Oxford: Pergamon Press, 1990.
29. M. Pourbaix, "Lectures on Electrochemical Corrosion," New York: Plenum Press, 1973.
30. C. Andrade, Cem. Concr. Res. 23 (1993): p.724.
31. R.K. Dhir, M.R. Jones, H.E.H. Ahmed, A.M.G. Seneviratne, Mag. Concr. Res. 42, 152 (1990): p. 177.
32. C. Andrade, J.M. Diez, A. Alaman, C. Alsono, Cem. Concr. Res. 25, 4 (1995): p. 727.
33. N.R. Buenfeld, S. El-Belbol, Mag. Concr. Res. 43, 155 (1991): p. 135.
34. C. Alonso, C. Andrade, J. Rodriguez, J.M. Diez, Mater. Struct. 31 (1998): p.435-441.
35. K.G.C. Berkeley, S. Pathmanaban, "Cathodic protection of reinforcement steel in concrete," London, Butterworth & Co.: 1990.
36. P.R. Vassie, "Non-destructive evaluation of the corrosion of concrete reinforcement by chlorides," in Proc. of symp. Corrosion of reinforcements in concrete construction, London, Society of chemical industry, 1979.
37. A. Bentur, S. Diamond, N.S. Berke, "Steel corrosion in concrete", London: E & FN Spon 1997.
38. W.D. Grimes, W.H. Hartt, D.H. Turner, Corrosion 35, 7 (1979): p.309.
39. RILEM Report, "Corrosion of Steel in Concrete", Ed. P. Schiessl, London: Chapman and Hall, 1988.
40. ACI 222R-96, "Corrosion of metals in concrete," ACI, 1997
41. M. Castellote, I. Llorente, C., Andrade, C., Alonso, Mater. Struct. 36 (2003): p.81.
42. J.A. Gonzalez, S. Feliu, P. Rodriquez, E. Ramirez, C. Alonso, C. Andrade, Mater. Struct. 29 (1996): p. 40.

List of Figures

Strength MPa	*Target Strength MPa*	*Cement*	*Water*	*Sand*	*Aggregate*
20	28	1	0.57	2.06	3.8
35	43	1	0.45	1.57	2.9
50	58	1	0.33	0.6	2.4

Table 1 Mix Proportions

Rebar Diameter (mm)	**Characteristic Strength MPa**	**Cover thickness (mm)**	**Actual Strength MPa**	**Dimensions (mm) w *x* h *x* L**
16	35	16	53	48x70x250
16	20	16	32	48x70x250
16	50	16	68	48x70x250
12	35	16	57	44x70x250
20	35	16	54	52x75x250
16	35	25	51	66x82x250
16	35	40	50	96x100x250

Table 2 Series description

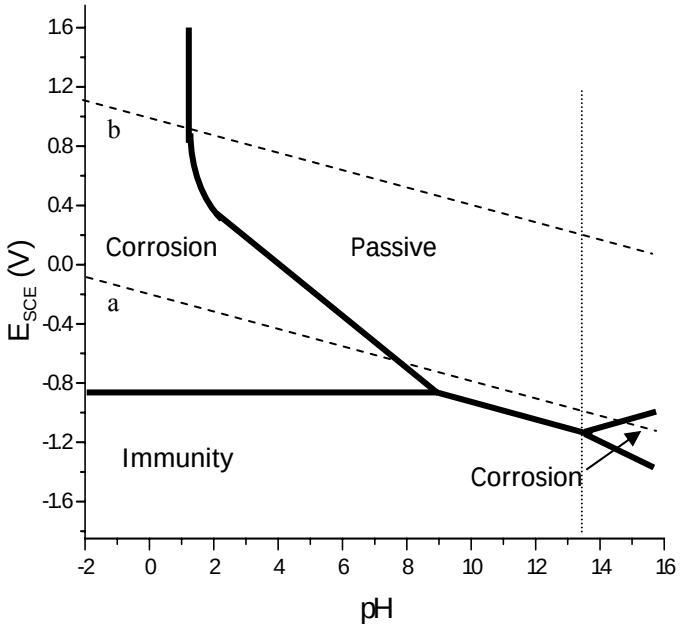

Figure 1 Potential-pH diagram for iron in water.

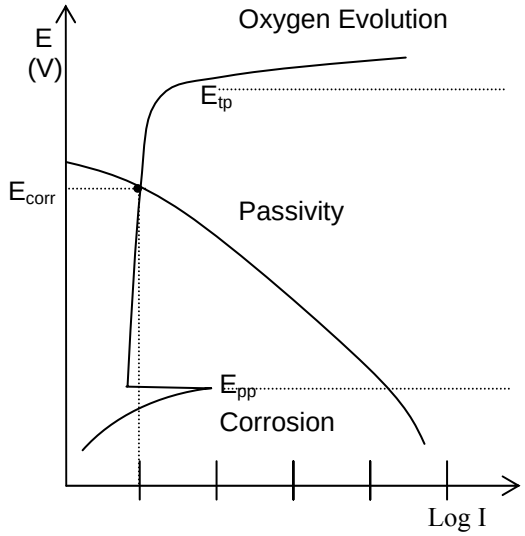

Figure 2a Schematic potentiostatic curve for steel in concrete, showing the mixed potential

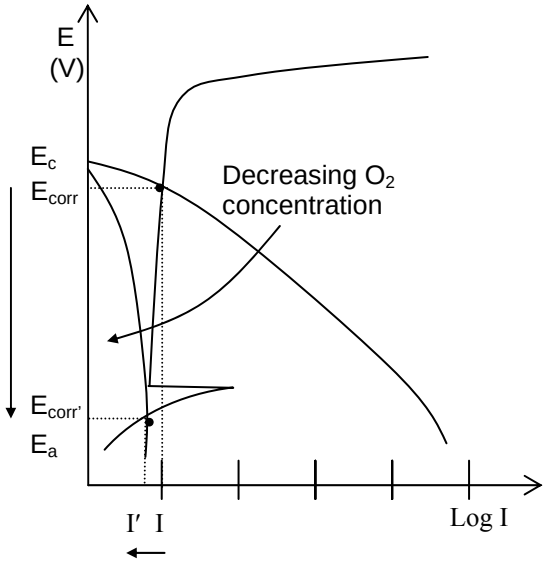

Figure 2b Effect of a decreasing oxygen concentration on the corrosion rate

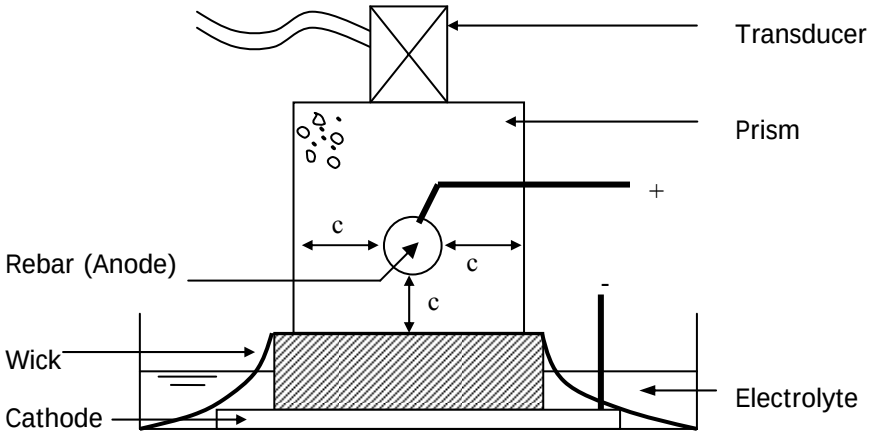

Figure 3 Accelerated corrosion cell

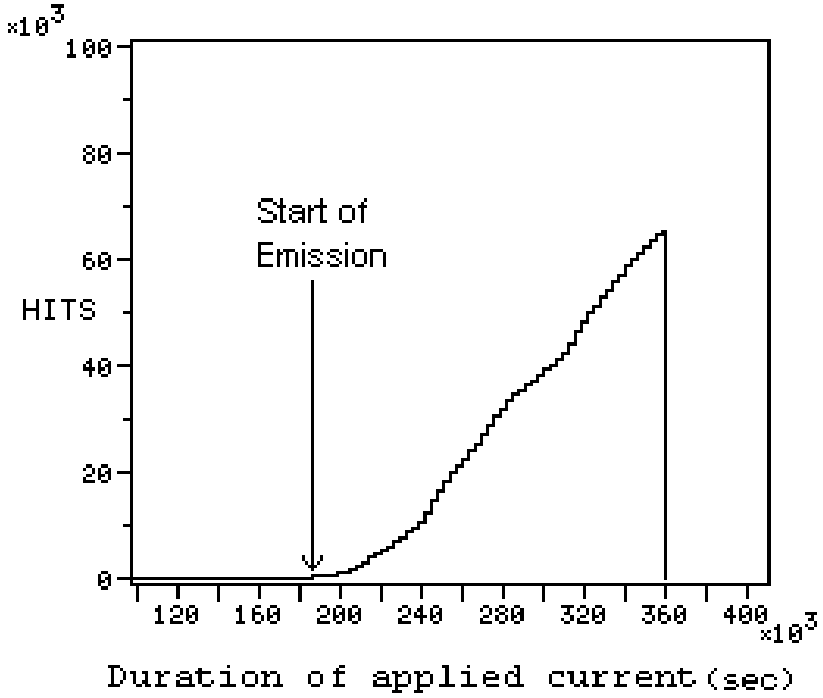

Figure 4 Increase in acoustic emission signifiying onset of corrosion (screen shot).

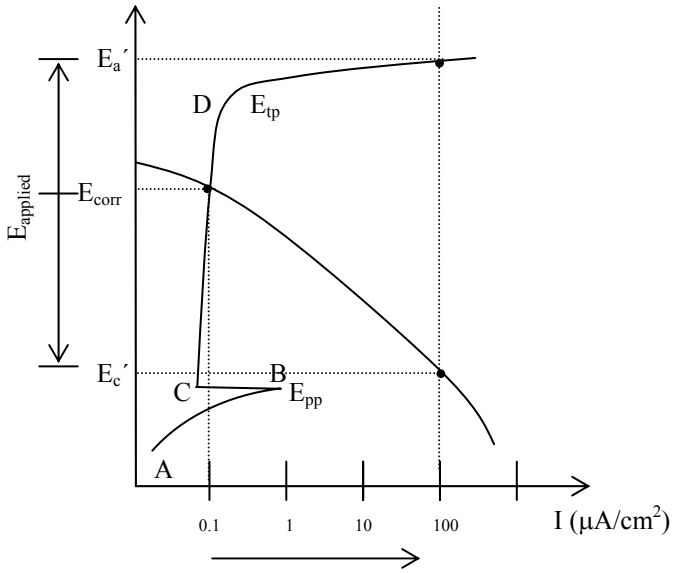

Figure 5 Change in potential required to achieve the desired current density

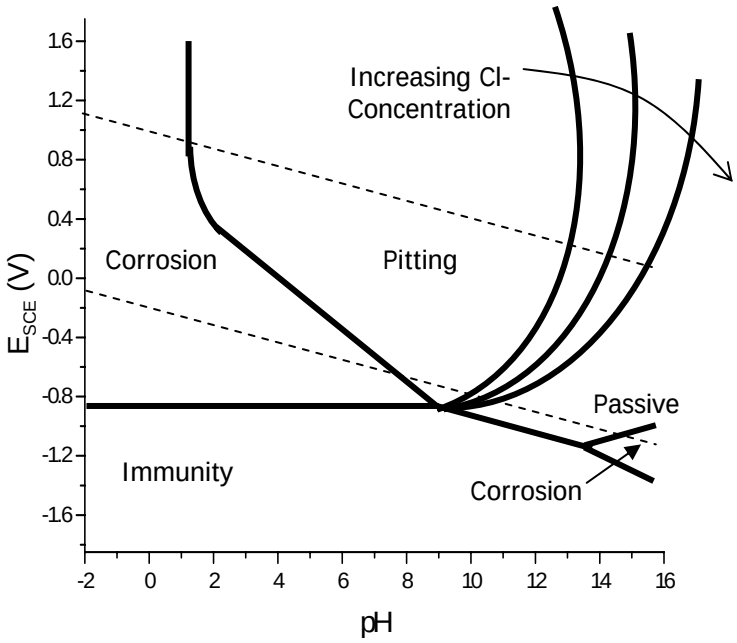

Figure 6 Potential – pH diagram for iron and water in the presence of chlorides

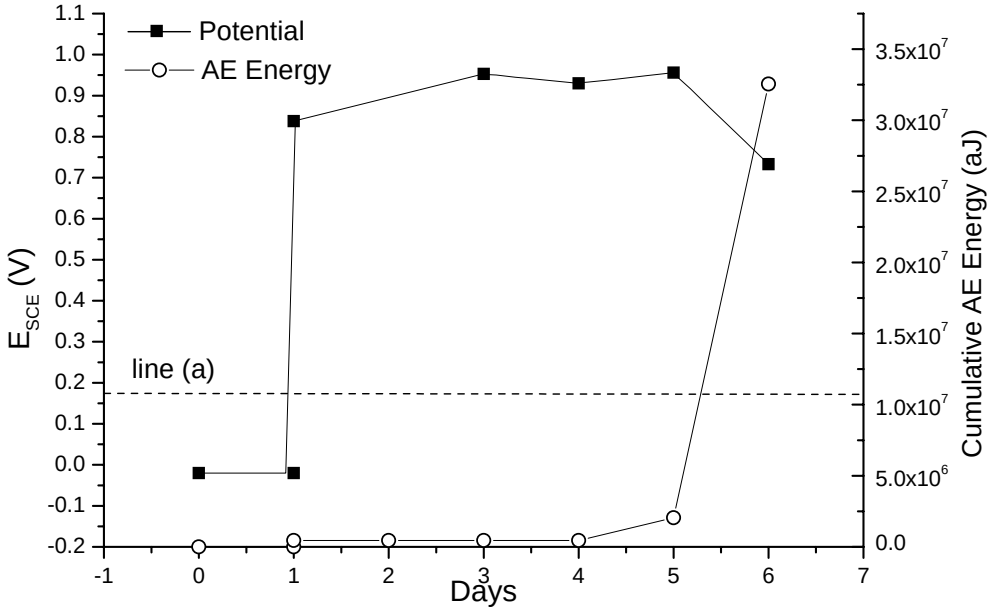

Figure 8 Typical half-cell potential and AE results

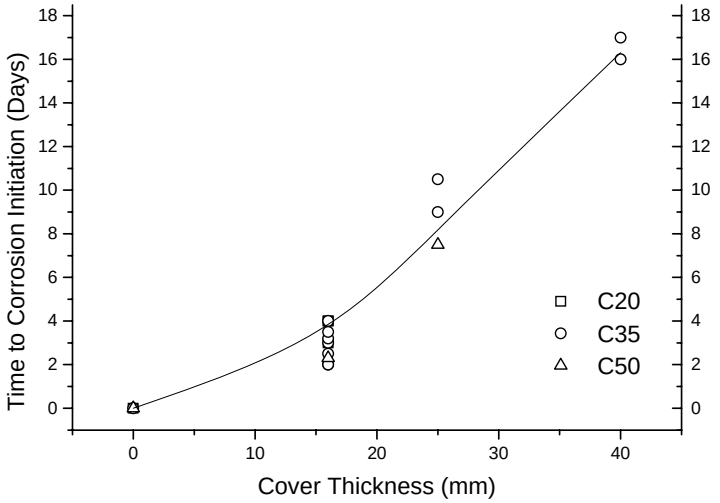

Figure 8 Time to corrosion initiation for various cover thickness' and strength combinations at 100 μA/cm^2

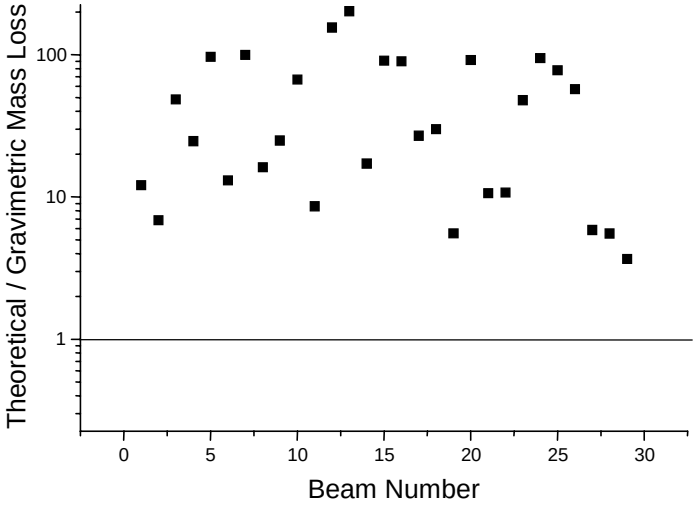

Figure 10 Mass loss ratio, not accounting for passivity

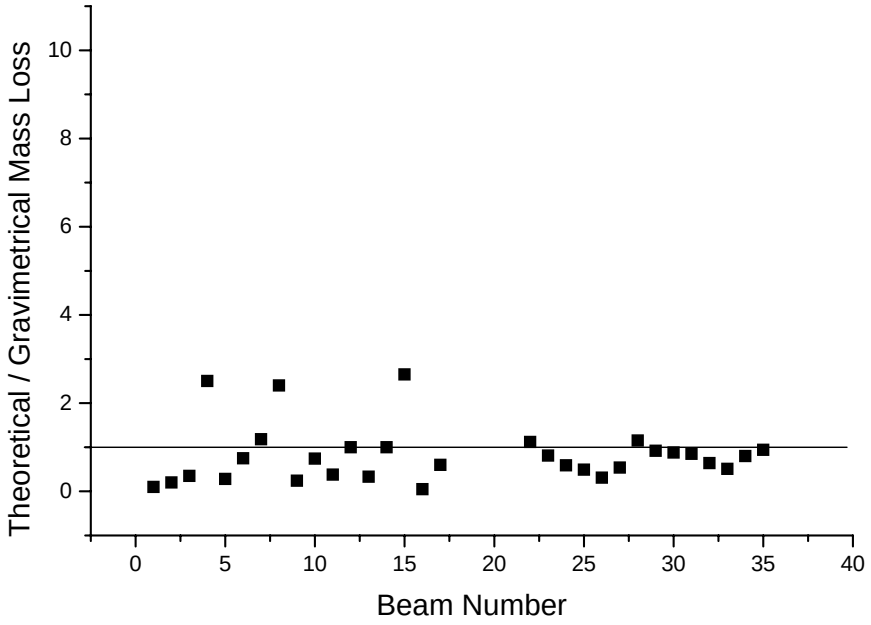

Figure 9 Mass loss ratio, accounting for passivity